
What If Without the Conformal Prediction Method

XIONG Zhixi

Department of Mathematics
Hong Kong University of Science and Technology
Hong Kong, China

Abstract

1 Introduction

In scientific, engineering, and everyday decision-making, obtaining a prediction is insufficient without also understanding its reliability through effective uncertainty quantification (UQ). Whether in autonomous driving, medical diagnosis, or financial risk assessment, relying solely on point estimates poses significant risks, as models are always imperfect and the world exhibits inherent noise. This challenge is formalized in classical decision theory, where optimal decisions require not only an expected outcome but a complete characterization of uncertainty. Formally, consider a decision problem where we observe data $x \in \mathcal{X}$ and must choose an action $a \in \mathcal{A}$. The consequence of this action depends on an unknown state $y \in \mathcal{Y}$, and is quantified by a loss function $L : \mathcal{A} \times \mathcal{Y} \rightarrow \mathbb{R}$. In the Bayesian decision theory [Berger, 1985], the optimal decision minimizes the *posterior expected loss*:

$$a^*(x) = \arg \min_{a \in \mathcal{A}} \mathbb{E}_{y \sim p(y|x)} [L(a, y)] = \arg \min_{a \in \mathcal{A}} \int_{\mathcal{Y}} L(a, y) p(y|x) dy, \quad (1)$$

where $p(y|x)$ is the posterior distribution of y given x . As shown in (1), the optimal action a^* depends not merely on a point estimate (such as the posterior mean), but on the entire posterior distribution. A poor characterization of $p(y|x)$ can lead to suboptimal decisions even with an accurate predictive model. Thus, robust and interpretable decision-making fundamentally requires well-calibrated uncertainty estimates. Consequently, a central challenge in modern machine learning, particularly for complex black-box models like deep neural networks, is to provide rigorous and reliable uncertainty measures for predictions. Without such measures, deploying these models in high-stakes domains remains risky.

To address this challenge, a variety of UQ methods have been developed, each with its own set of limitations that restrict practical applicability. Parametric models, for instance, often rely on strong distributional assumptions (e.g., normality) that are rarely justified in complex, real-world data settings [Wasserman, 2004]. Asymptotic theories, while providing theoretical guarantees under ideal conditions, require sample sizes that are often unattainable in practice, and their convergence may not be guaranteed for finite or moderate datasets [Vovk et al., 2005]. Within the Bayesian paradigm, the choice of a prior distribution can be subjective and difficult to justify. Furthermore, computing the posterior distribution is often intractable for high-dimensional or non-conjugate models, which often necessitates the use of approximate inference schemes that may themselves introduce errors [Murphy, 2012]. Among more recent machine learning approaches, ensemble methods (e.g., deep ensembles [Lakshminarayanan et al., 2017]) can yield well-calibrated uncertainty estimates but at a prohibitive computational cost, as they require training and maintaining multiple models, which is a significant burden for large datasets and complex architectures. Techniques like Monte Carlo Dropout [Gal and Ghahramani, 2016] offer a more lightweight alternative by approximating Bayesian inference within neural networks, yet they impose specific architectural constraints (e.g., dropout layers) and require careful tuning of key hyperparameters, most notably the dropout rate,

as well as the overall training schedule. Lastly, generative models (e.g., diffusion [Ho et al., 2020] or flow matching [Lipman et al., 2022]) can model complex data distributions but are notoriously expensive to train and may be challenging to scale to high-dimensional problems. In summary, existing methods are often constrained by strong assumptions, high computational demands, or a lack of finite-sample guarantees, highlighting the need for a framework that is both model-agnostic and theoretically rigorous.

The conformal prediction (CP) framework emerges as a compelling solution to these limitations, offering a model-agnostic approach to UQ with finite-sample, distribution-free guarantees [Gammerman et al., 1998, Vovk et al., 2005]. Its core mechanism relies on the concept of *nonconformity scores*. For any new input, CP evaluates how nonconforming each potential output appears relative to a set of labeled reference (or calibration) data. By calibrating a threshold based on the empirical distribution of these scores, CP constructs a prediction set (for classification) or a prediction interval (for regression) that is guaranteed to contain the true outcome with a user-specified probability (e.g., 90%), under the weak assumption of data exchangeability. This procedure essentially uses past empirical errors to quantify future uncertainty, requiring no strong distributional assumptions, no modifications to the underlying model, and no asymptotic approximations.

Originally introduced by Gammerman, Vovk, and Vapnik in 1998 for Support Vector Machines [Hearst et al., 1998], Conformal Prediction has transcended its initial scope to become a pervasive framework in modern reliable AI. While theoretically grounded, its value is most evident in its rapidly expanding real-world impact across diverse high-stakes domains. In the natural sciences, CP is now pivotal for guiding protein design sequences [Fannjiang et al., 2022]. In the realm of robotics and embodied AI, it facilitates safe planning in dynamic environments [Lindemann et al., 2023] and has been successfully applied to align uncertainty in Large Language Models (LLMs) for robotic interaction [Ren et al., 2023]. The framework’s reliability is equally critical in healthcare, where it has been deployed for estimating diagnostic uncertainty in cancer pathology [Olsson et al., 2022] and predicting disease courses for conditions such as multiple sclerosis [Sreenivasan et al., 2025]. Additionally, CP has found utility in earth observation [Singh et al., 2024], further demonstrating its versatility and robustness in securing trust for safety-critical applications. Collectively, these advancements illustrate the transformative potential of CP in bridging the gap between complex, black-box algorithms and the rigorous safety standards demanded by real-world applications.

2 Methods

This section formalizes the CP framework. We begin with the general transductive formulation, proceed to the computationally efficient Split Conformal Prediction, and conclude by discussing advanced variants designed to address limitations regarding adaptivity, distribution shifts, and conditional coverage.

2.1 General Conformal Prediction Framework

Consider a regression or classification problem where we observe a sequence of data points Z_1, \dots, Z_n , where $Z_i = (X_i, Y_i) \in \mathcal{X} \times \mathcal{Y}$. We assume these data points are *exchangeable*, meaning their joint distribution is invariant under any permutation. Given a new test input X_{n+1} , our goal is to construct a prediction set $C(X_{n+1}) \subseteq \mathcal{Y}$ that covers the unknown true label Y_{n+1} with a user-specified probability $1 - \alpha$, where $\alpha \in (0, 1)$ is the miscoverage rate.

The general conformal prediction framework, often referred to as Full or Transductive CP [Vovk et al., 2005], relies on a *nonconformity measure* $S : \mathcal{Z} \rightarrow \mathbb{R}$. This function assigns a score $s_i = S(Z_i)$ representing how “unusual” a data point Z_i is relative to the others. For a candidate label $y \in \mathcal{Y}$ paired with X_{n+1} , we form a hypothetical dataset including $Z_{n+1} = (X_{n+1}, y)$. We then compute nonconformity scores for all $i \in \{1, \dots, n+1\}$. A p -value for the candidate y is derived by comparing its score to the scores of the existing data:

$$\pi(y) = \frac{1}{n+1} \sum_{i=1}^{n+1} \mathbb{I}(s_i \geq s_{n+1}), \quad (2)$$

where $\mathbb{I}(\cdot)$ is the indicator function. The prediction set is constructed by including all candidates y that appear statistically plausible:

$$C_{\text{Full}}(X_{n+1}) = \{y \in \mathcal{Y} \mid \pi(y) > \alpha\}. \quad (3)$$

Under the exchangeability assumption, this set satisfies the marginal validity property:

$$\mathbb{P}(Y_{n+1} \in C_{\text{Full}}(X_{n+1})) \geq 1 - \alpha, \quad (4)$$

for any sample size n and any underlying distribution. The structure of the set $C_{\text{Full}}(X_{n+1})$ depends on the nature of the output space \mathcal{Y} :

Classification. When \mathcal{Y} is a finite set of discrete labels (e.g., $\{1, \dots, K\}$), we can explicitly calculate $\pi(y)$ for each possible class. The prediction set is simply the subset of labels for which the p -value exceeds α .

Regression. When $\mathcal{Y} = \mathbb{R}$, iterating through all possible values of y is computationally impossible. However, for standard nonconformity measures (such as the absolute error $|y - \hat{\mu}(X_{n+1})|$), the function $\pi(y)$ is generally quasi-concave with respect to y . Consequently, the set defined in (3) typically forms a continuous interval (or a union of intervals). In practice, this interval is computed by inverting the nonconformity score function to find the boundaries of y that satisfy the condition $\pi(y) > \alpha$.

2.2 Split Conformal Prediction

While theoretically robust, Full CP is computationally prohibitive for complex models (e.g., neural networks) because it requires retraining the underlying model for every candidate y to compute the scores s_i properly. To address this computational bottleneck, *Split Conformal Prediction* (SCP), also known as Inductive CP, is the most widely adopted variant in modern machine learning [Papadopoulos et al., 2002, Lei et al., 2018].

In SCP, the available data is partitioned into two disjoint subsets: a proper training set $\mathcal{D}_{\text{train}}$ and a calibration set $\mathcal{D}_{\text{cal}} = \{(X_i, Y_i)\}_{i=1}^n$. A predictive model is trained solely on $\mathcal{D}_{\text{train}}$. We then compute nonconformity scores on \mathcal{D}_{cal} using this fixed model. The construction of the prediction set depends on the task type:

Classification. For a classification task with discrete labels $\mathcal{Y} = \{1, \dots, K\}$, the model $\hat{f} : \mathcal{X} \rightarrow [0, 1]^K$ typically outputs a probability distribution over classes, where $\hat{f}(x)_k$ denotes the estimated probability of class k . A common nonconformity score is the complement of the probability assigned to the true class:

$$s_i = 1 - \hat{f}(X_i)_{Y_i}, \quad \forall i \in \mathcal{D}_{\text{cal}}. \quad (5)$$

Let \hat{q} be the $\lceil (n+1)(1-\alpha) \rceil / n$ empirical quantile of the calibration scores $\{s_1, \dots, s_n\}$. The prediction set includes all classes with a predicted probability above the calibrated threshold:

$$C_{\text{SCP}}(X_{n+1}) = \left\{ k \in \mathcal{Y} \mid \hat{f}(X_{n+1})_k \geq 1 - \hat{q} \right\}. \quad (6)$$

This formulation, often referred to as Least Ambiguous Set-valued Classifiers [Sadinle et al., 2019], guarantees that the true label is included in the set with probability at least $1 - \alpha$.

Regression. For a regression task ($\mathcal{Y} = \mathbb{R}$), let $\hat{\mu} : \mathcal{X} \rightarrow \mathbb{R}$ be the trained model. A standard choice for the nonconformity score is the absolute residual:

$$s_i = |Y_i - \hat{\mu}(X_i)|, \quad \forall i \in \mathcal{D}_{\text{cal}}. \quad (7)$$

Similarly, let \hat{q} be the $\lceil (n+1)(1-\alpha) \rceil / n$ empirical quantile of these regression scores. The prediction set for a new input X_{n+1} is constructed as a fixed-width interval:

$$C_{\text{SCP}}(X_{n+1}) = [\hat{\mu}(X_{n+1}) - \hat{q}, \quad \hat{\mu}(X_{n+1}) + \hat{q}]. \quad (8)$$

In both cases, SCP maintains the finite-sample validity guarantee provided the calibration and test data are exchangeable. Because the model is trained only once, SCP is computationally efficient and model-agnostic.

2.3 Advanced Variants addressing Limitations

While SCP establishes a rigorous baseline for UQ, its standard formulation exhibits three significant limitations when applied to complex, real-world scenarios. First, the reliance on a global threshold produces prediction sets of fixed size (e.g., fixed-width intervals), failing to account for *heteroscedasticity* where uncertainty varies locally across the input space. Second, the theoretical validity of SCP hinges on the assumption of exchangeability, which is often violated under *covariate shifts* (e.g., distribution shift). Third, SCP only guarantees *marginal* coverage averaged over the entire population, which permits systematic under-coverage for specific subgroups or minority classes. To address these challenges, several specialized variants have been developed.

Heteroscedasticity and Locally Adaptive Conformal Prediction. Standard SCP constructs prediction intervals of fixed width $2\hat{q}$ across the entire input space. This approach assumes homoscedasticity and results in inefficiency: the intervals are unnecessarily wide for “easy” inputs and potentially too narrow for “hard” ones. To address this, *Conformalized Quantile Regression* (CQR) [Romano et al., 2019] was proposed to construct intervals that adapt their width to the local difficulty of the input. The CQR procedure consists of two main steps: quantile regression training and conformal calibration.

First, using the training set $\mathcal{D}_{\text{train}}$, we train a regression model \hat{f} to estimate two conditional quantiles: the lower quantile at level $\gamma_{\text{lo}} = \alpha/2$ and the upper quantile at level $\gamma_{\text{hi}} = 1 - \alpha/2$. The model outputs $\hat{q}_{\text{lo}}(x)$ and $\hat{q}_{\text{hi}}(x)$, which are optimized by minimizing the pinball loss (or quantile loss) [Koenker and Hallock, 2001]:

$$\mathcal{L}(y, \hat{y}, \gamma) = \max(\gamma(y - \hat{y}), (\gamma - 1)(y - \hat{y})). \quad (9)$$

The total objective minimizes the average loss over both quantiles: $\sum_{i \in \mathcal{D}_{\text{train}}} [\mathcal{L}(y_i, \hat{q}_{\text{lo}}(x_i), \gamma_{\text{lo}}) + \mathcal{L}(y_i, \hat{q}_{\text{hi}}(x_i), \gamma_{\text{hi}})]$.

Second, although these raw quantile estimates provide a heuristic interval $[\hat{q}_{\text{lo}}(X), \hat{q}_{\text{hi}}(X)]$, they do not guarantee finite-sample coverage. CQR acts as a “wrapper” to rigorously calibrate them. We compute nonconformity scores on the calibration set \mathcal{D}_{cal} as:

$$s_i = \max(\hat{q}_{\text{lo}}(X_i) - Y_i, Y_i - \hat{q}_{\text{hi}}(X_i)). \quad (10)$$

Intuitively, s_i measures the signed distance from the true label Y_i to the nearest boundary of the predicted interval. If Y_i falls inside the interval, s_i is negative; if it falls outside, s_i is positive.

Let \hat{q} be the $\lceil (n+1)(1-\alpha) \rceil / n$ empirical quantile of these scores $\{s_1, \dots, s_n\}$. The final conformalized prediction interval for a new input X_{n+1} is constructed by expanding (or shrinking) the raw quantile estimates by \hat{q} :

$$C_{\text{CQR}}(X_{n+1}) = [\hat{q}_{\text{lo}}(X_{n+1}) - \hat{q}, \hat{q}_{\text{hi}}(X_{n+1}) + \hat{q}]. \quad (11)$$

This procedure ensures valid coverage while allowing the interval width $\hat{q}_{\text{hi}}(X) - \hat{q}_{\text{lo}}(X) + 2\hat{q}$ to vary dynamically based on the input X , significantly improving informativeness in heteroscedastic settings.

Covariate Shift and Weighted Conformal Prediction. The standard exchangeability assumption is violated under distribution shift, where the test distribution $P_{\text{test}}(X)$ differs from the training distribution $P_{\text{train}}(X)$. Under such *covariate shift*, standard CP loses its coverage guarantee. Tibshirani et al. [2019] proposed *Weighted Conformal Prediction* (WCP), which adjusts the quantile calculation using likelihood ratios. For each calibration point $X_i \in \mathcal{D}_{\text{cal}}$, we assign a weight proportional to the density ratio:

$$w(X_i) = \frac{dP_{\text{test}}(X_i)}{dP_{\text{train}}(X_i)} = \frac{p_{\text{test}}(X_i)}{p_{\text{train}}(X_i)}, \quad (12)$$

where p_{test} and p_{train} denote the probability density functions (or probability mass functions) of the test and training distributions, respectively. Intuitively, $w(X_i)$ quantifies how much more likely the input X_i is to appear in the test environment compared to the training environment.

Given these weights, WCP modifies the standard calibration procedure by replacing the uniform empirical distribution with a weighted counterpart. Specifically, after computing nonconformity scores $\{s_i\}_{i=1}^n$ on the calibration set, we assign a normalized probability mass to each point. For a new test

input X_{n+1} , the calibration points are weighted by $w(X_i)$, while the test point itself is assigned a fixed weight of 1 (reflecting its draw from the target distribution). The resulting probability weights are defined as:

$$p_i(X_{n+1}) = \frac{w(X_i)}{\sum_{j=1}^n w(X_j) + 1}, \quad p_{n+1}(X_{n+1}) = \frac{1}{\sum_{j=1}^n w(X_j) + 1}. \quad (13)$$

These probabilities are then used to construct the weighted empirical cumulative distribution function of the scores:

$$\hat{F}(s) = \sum_{i=1}^n p_i(X_{n+1}) \mathbb{I}(s_i \leq s) + p_{n+1}(X_{n+1}) \mathbb{I}(\infty \leq s). \quad (14)$$

The calibrated threshold \hat{q} is determined as the smallest score s such that $\hat{F}(s) \geq 1 - \alpha$. Consequently, the final prediction set is formed as $C_{\text{WCP}}(X_{n+1}) = [\hat{u}(X_{n+1}) - \hat{q}, \hat{u}(X_{n+1}) + \hat{q}]$. By incorporating the likelihood ratio into the quantile estimation, this method ensures that the coverage guarantee holds with respect to the target distribution P_{test} .

Conditional Coverage and Mondrian Conformal Prediction. Standard SCP guarantees *marginal* coverage, meaning $\mathbb{P}(Y \in C(X)) \geq 1 - \alpha$ on average over the entire population. However, this global guarantee allows for systematic under-coverage in specific subgroups (e.g., minority classes or difficult input regions) as long as it is compensated by over-coverage elsewhere. To address this, *Mondrian Conformal Prediction* (MCP) [Vovk et al., 2005] enforces validity within defined categories.

Let $K : \mathcal{X} \rightarrow \{1, \dots, M\}$ be a taxonomy function that maps an input X to one of M categories (or “bins”). We partition the calibration set \mathcal{D}_{cal} into disjoint subsets based on these categories:

$$\mathcal{D}_{\text{cal}}^{(m)} = \{(X_i, Y_i) \in \mathcal{D}_{\text{cal}} \mid K(X_i) = m\}, \quad \text{for } m = 1, \dots, M. \quad (15)$$

Calibration is then performed independently within each bin. For a new test input X_{n+1} belonging to category $m^* = K(X_{n+1})$, we compute the nonconformity scores using only the data in $\mathcal{D}_{\text{cal}}^{(m^*)}$. Let $n_{m^*} = |\mathcal{D}_{\text{cal}}^{(m^*)}|$ be the number of calibration samples in this category. We calculate the category-specific quantile $\hat{q}_{1-\alpha}^{(m^*)}$ as the $\lceil (n_{m^*} + 1)(1 - \alpha) \rceil / n_{m^*}$ empirical quantile of the scores in $\mathcal{D}_{\text{cal}}^{(m^*)}$. The prediction set is then constructed as:

$$C_{\text{MCP}}(X_{n+1}) = \left\{ y \in \mathcal{Y} \mid S((X_{n+1}, y)) \leq \hat{q}_{1-\alpha}^{(m^*)} \right\}. \quad (16)$$

By stratifying the calibration process, MCP ensures that the coverage guarantee holds conditionally for each group:

$$\mathbb{P}(Y_{n+1} \in C_{\text{MCP}}(X_{n+1}) \mid K(X_{n+1}) = m) \geq 1 - \alpha, \quad \forall m \in \{1, \dots, M\}. \quad (17)$$

This property is particularly vital in safety-critical applications where fairness across subgroups or reliability across different operating modes is required.

3 Advantages and Impact

The CP framework offers a rigorous alternative to traditional UQ methods. Its rising popularity in statistical machine learning is driven by several distinctive advantages that address the limitations of parametric and asymptotic approaches.

3.1 Finite-Sample Coverage

A defining characteristic of CP is its validity for any finite sample size n . Unlike asymptotic statistical theories, which guarantee coverage only as $n \rightarrow \infty$, CP ensures that the constructed prediction sets cover the true outcome with probability at least $1 - \alpha$ even when the number of available data points is small. This finite-sample validity is derived directly from the randomization of the data sequence and does not rely on large-sample approximations. This property is particularly vital in

domains where data collection is expensive or scarce, ensuring that the reported confidence levels are trustworthy regardless of dataset size.

To empirically validate this theoretical guarantee, particularly in data-scarce regimes, we conducted a comparative experiment using the Diabetes dataset. We employed Gradient Boosting Quantile Regression (QR) as the base model to predict disease progression based on BMI and other features. The data was partitioned to simulate a small-sample setting with a calibration set of only $N_{\text{cal}} = 50$ samples. We compared the “Raw” output of the quantile regressors against the CQR method, targeting a 90% coverage rate ($\alpha = 0.1$).

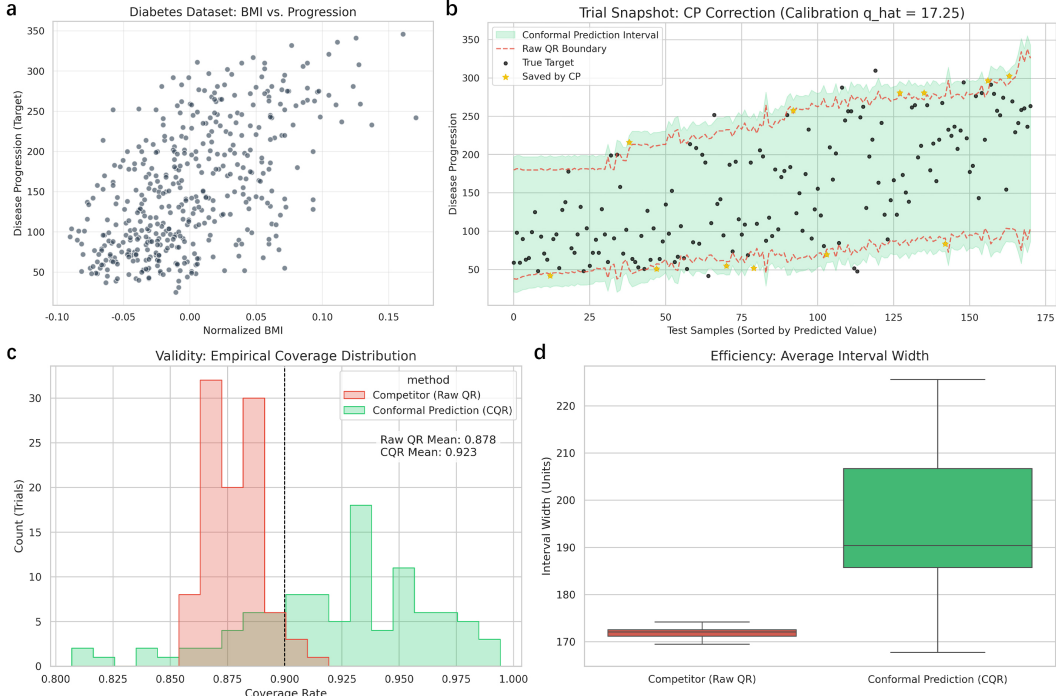


Figure 1: Validation of Finite-Sample Guarantee on the Diabetes Dataset. (a) The distribution of the dataset (BMI vs. Target). (b) A snapshot of a single trial comparing Raw QR bounds (red dashed lines) with CP intervals (green band). The yellow stars indicate test points that fell outside the raw model’s bounds but were successfully captured by the CP correction (\hat{q} adjustment). (c) Distribution of empirical coverage rates over 100 trials. The Raw QR method (red) consistently under-covers (mean $\approx 87.8\%$), failing to meet the 90% target (dashed line) due to finite-sample errors. In contrast, CQR (green) rigorously satisfies the validity property (mean $\approx 92.3\%$). (d) The boxplot of interval widths shows that CP achieves validity by appropriately expanding the intervals to account for the uncertainty inherent in the small calibration set.

The results, visualized in Figure 1, clearly demonstrate the risks of relying on asymptotic approximations when sample sizes are finite. As shown in Panel (c), the Raw QR (competitor) consistently fails to meet the user-specified 90% confidence level, achieving an average coverage of only 87.8%. This under-coverage occurs because the asymptotic assumptions of the quantile loss do not hold for $N_{\text{cal}} = 50$.

In contrast, the Conformal Prediction method corrects these errors. By computing a calibrated adjustment factor \hat{q} based on the empirical distribution of nonconformity scores, CP ensures the target coverage is met (average 92.3%). Panel (b) illustrates the mechanism: the CP intervals (green band) dynamically expand beyond the raw model predictions (red dashed lines) to capture “hard” examples (marked with yellow stars), effectively acting as a safety net. While this correction results in slightly wider intervals (Panel d), it is a necessary trade-off to guarantee reliability in safety-critical or data-limited applications.

3.2 Distribution-Free

CP is inherently distribution-free, meaning its validity holds for any underlying joint distribution P_{XY} , provided the data points are exchangeable. Traditional parametric methods often rely on strong assumptions, such as the normality of error terms (Gaussianity), which are frequently violated in complex, real-world high-dimensional data. CP requires no knowledge of the generative process and no estimation of density functions. By relying solely on the exchangeability assumption (which is satisfied by i.i.d. data), CP remains robust even in the presence of heavy tails or skewness.

To demonstrate this robustness against non-standard distributions, we performed an experiment using synthetic data with explicitly non-Gaussian noise. We generated a non-linear regression dataset and added skewed noise drawn from an exponential distribution (centered to zero). This setup mimics real-world scenarios where error terms are asymmetric and heavy-tailed, violating the standard Gaussian assumption utilized by many parametric methods. We trained a neural network regressor and compared a baseline Gaussian uncertainty estimation ($\text{Mean} \pm 1.64\sigma$) against CP, both targeting a 90% coverage rate.

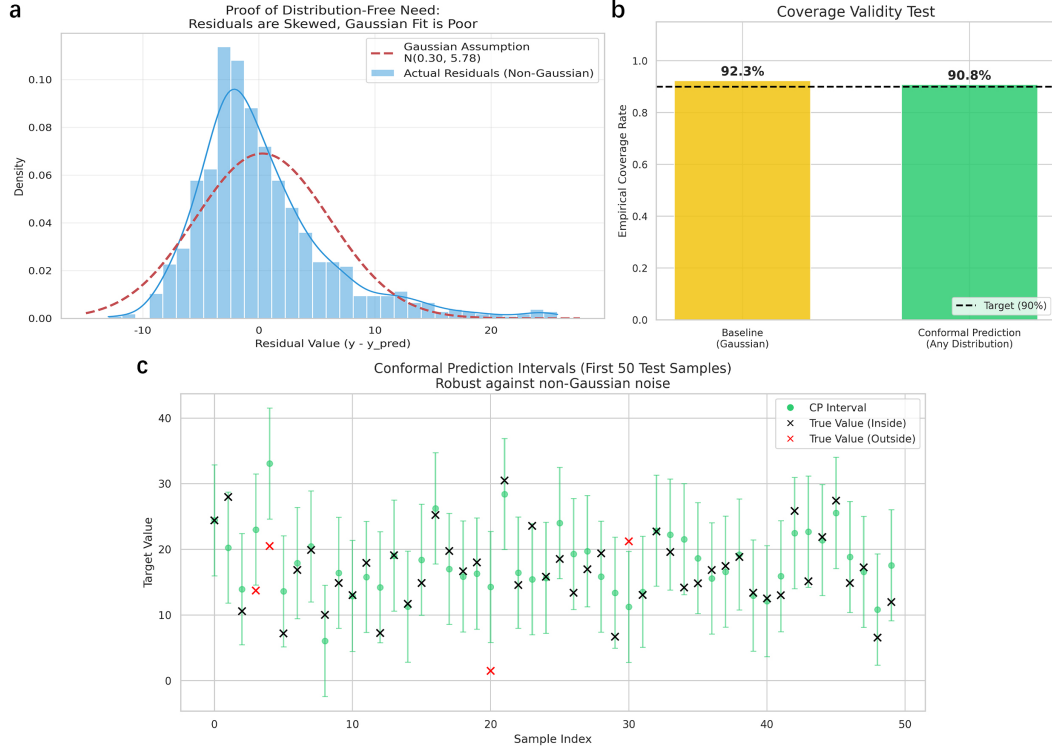


Figure 2: Validation of Distribution-Free Robustness. (a) Histogram of the actual residuals (blue) versus the Gaussian fit (red dashed line) assumed by the baseline method. The clear skewness and heavy tail of the actual data violate the normality assumption, leading to a poor fit. (b) Comparison of empirical coverage rates. The Gaussian baseline (yellow) fails to capture the true distribution's shape, resulting in unpredictable coverage. In contrast, CP (green) achieves near-perfect validity (90.8%) by relying on the empirical quantiles of the residuals rather than a density estimate. (c) Visualization of CP intervals for the first 50 test samples. The intervals (green bars) effectively contain the true targets (black crosses) even in the presence of asymmetric noise, with failures (red crosses) occurring at the expected rate of $\alpha = 10\%$.

The results, shown in Figure 2, underscore the necessity of distribution-free methods. Panel (a) reveals the significant discrepancy between the actual skewed residuals (blue histogram) and the fitted Gaussian distribution (red dashed line). Because the baseline method assumes symmetry and thin tails, it cannot accurately model the risk. Consequently, as shown in Panel (b), the baseline achieves an arbitrary coverage rate that may not align with the safety requirement.

However, CP remains unaffected by the skewness. By computing the nonconformity scores directly from the data and determining the threshold empirically (Panel c), it achieves a coverage of 90.8%, aligning almost perfectly with the target. This confirms that CP provides valid UQ for arbitrary data distributions without requiring feature engineering or complex density estimation.

3.3 Model-Free

The CP framework, particularly the Split CP formulation, is fully model-agnostic. It operates as a “wrapper” around any predictive model, decoupling the task of UQ from model training. Whether the underlying predictor is a simple linear regression or a massive deep neural network, CP can calibrate its outputs without requiring modifications to the model architecture, loss function, or optimization procedure. This contrasts significantly with Bayesian Neural Networks or Deep Ensembles, which often impose specific structural constraints or incur prohibitive computational costs. This flexibility allows researchers to equip state-of-the-art “black-box” models with rigorous uncertainty estimates efficiently.

To rigorously verify the model-agnostic property of the CP framework, we conducted a comprehensive experiment using the *Concrete Compressive Strength* dataset. We employed seven distinct machine learning architectures spanning the major paradigms of regression: Instance-based (KNN), Linear (Ridge), Tree-based (Decision Tree), Kernel-based (SVR), Ensemble methods (Random Forest, Gradient Boosting), and Deep Learning (Neural Network). The target miscoverage rate was set to $\alpha = 0.1$ (90% confidence).

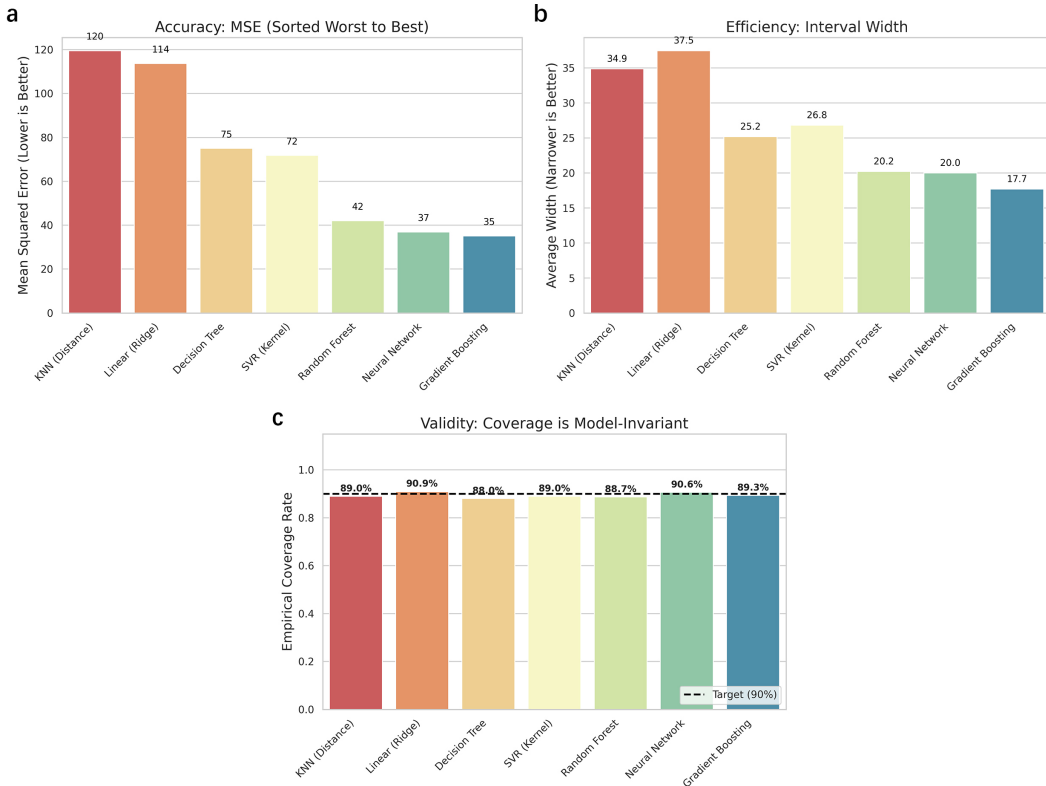


Figure 3: Evaluation of Model Agnosticism across 7 Architectures. (a) Models sorted by predictive error (MSE), ranging from weaker models (KNN, Linear) to strong ensembles (Gradient Boosting). (b) The average prediction interval width follows the trend of the MSE. Stronger models like Gradient Boosting produce significantly sharper intervals (17.7 units) compared to the Linear baseline (37.5 units). (c) Empirical coverage rates for all models. Despite the vast differences in underlying mathematical principles and accuracy, CP ensures that every model approximates the 90% target (dashed line), validating the model-free property.

First, validity is invariant to model choice. As shown in Panel (c), all seven models achieve empirical coverage rates close to the nominal 90% level, regardless of whether the model is a simple linear equation or a complex non-linear ensemble. It is worth noting that some methods, such as the Decision Tree (88.0%) or Random Forest (88.7%), exhibit coverage slightly below the exact 90% threshold. This does not indicate a failure of the method. The coverage guarantee provided by Split Conformal Prediction is marginal ($1 - \alpha$) over the randomness of the calibration/test split. For any finite test set size N_{test} , the observed coverage follows a binomial distribution around $1 - \alpha$. Therefore, minor fluctuations (e.g., $\pm 2\%$) are expected statistical noise inherent to finite-sample evaluation, not a violation of the theoretical validity.

Second, accuracy translates to efficiency. Panels (a) and (b) demonstrate the clear advantage of using high-performance models. There is a clear correlation between the Mean Squared Error and the average interval width. The *Gradient Boosting* regressor, which achieves the lowest error (MSE ≈ 35), produces the sharpest uncertainty estimates with an average width of 17.7 units. In contrast, the *Linear Ridge* model (MSE ≈ 114) requires intervals more than twice as wide (37.5 units) to achieve the same 90% safety guarantee. This confirms that while CP acts as a universal safety net, improving the underlying “black-box” model directly rewards the user with more informative and actionable prediction sets.

Collectively, these advantages have positioned CP as a cornerstone of modern reliable AI. By providing a framework that is theoretically rigorous yet practically implementable, CP has bridged the gap between abstract statistical guarantees and high-stakes applications. It has enabled safe decision-making in fields such as medical diagnostics, where “knowing what the model doesn’t know” is as critical as prediction accuracy. Furthermore, it has spurred a new direction of research focused on distribution shifts and fairness, ensuring that machine learning systems remain safe and robust in dynamic, open-world environments.

4 Comparative Analysis

5 Conclusion

References

- JO Berger. Statistical decision theory and bayesian analysis. *Springer series in statistics Show all parts in this series*, 1985.
- Clara Fannjiang, Stephen Bates, Anastasios N Angelopoulos, Jennifer Listgarten, and Michael I Jordan. Conformal prediction under feedback covariate shift for biomolecular design. *Proceedings of the National Academy of Sciences*, 119(43):e2204569119, 2022.
- Yarin Gal and Zoubin Ghahramani. Dropout as a bayesian approximation: Representing model uncertainty in deep learning. In *international conference on machine learning*, pages 1050–1059. PMLR, 2016.
- A. Gammerman, V. Vovk, and V. Vapnik. Learning by transduction. In *Proceedings of the Fourteenth Conference on Uncertainty in Artificial Intelligence*, UAI’98, page 148–155, San Francisco, CA, USA, 1998. Morgan Kaufmann Publishers Inc. ISBN 155860555X.
- Marti A. Hearst, Susan T Dumais, Edgar Osuna, John Platt, and Bernhard Scholkopf. Support vector machines. *IEEE Intelligent Systems and their applications*, 13(4):18–28, 1998.
- Jonathan Ho, Ajay Jain, and Pieter Abbeel. Denoising diffusion probabilistic models. *Advances in neural information processing systems*, 33:6840–6851, 2020.
- Roger Koenker and Kevin F Hallock. Quantile regression. *Journal of economic perspectives*, 15(4):143–156, 2001.
- Balaji Lakshminarayanan, Alexander Pritzel, and Charles Blundell. Simple and scalable predictive uncertainty estimation using deep ensembles. In *Advances in neural information processing systems*, volume 30, 2017.
- Jing Lei, Max G’Sell, Alessandro Rinaldo, Ryan J Tibshirani, and Larry Wasserman. Distribution-free predictive inference for regression. *Journal of the American Statistical Association*, 113(523):1094–1111, 2018.

- Lars Lindemann, Matthew Cleaveland, Gihyun Shim, and George J Pappas. Safe planning in dynamic environments using conformal prediction. *IEEE Robotics and Automation Letters*, 8(8):5116–5123, 2023.
- Yaron Lipman, Ricky TQ Chen, Heli Ben-Hamu, Maximilian Nickel, and Matt Le. Flow matching for generative modeling. *arXiv preprint arXiv:2210.02747*, 2022.
- Kevin P Murphy. *Machine Learning: A Probabilistic Perspective*. MIT press, 2012.
- Henrik Olsson, Kimmo Kartasalo, Nita Mulliqi, Marco Capuccini, Pekka Ruusuvuori, Hemamali Samaratunga, Brett Delahunt, Cecilia Lindskog, Emiel AM Janssen, Anders Blilie, et al. Estimating diagnostic uncertainty in artificial intelligence assisted pathology using conformal prediction. *Nature communications*, 13(1):7761, 2022.
- Harris Papadopoulos, Kyriakos Proedrou, Volodya Vovk, and Alex Gammerman. Inductive confidence machines for regression. In *European Conference on Machine Learning*, pages 345–356. Springer, 2002.
- Allen Z Ren, Anushri Dixit, Alexandra Bodrova, Sumeet Singh, Stephen Tu, Noah Brown, Peng Xu, Leila Takayama, Fei Xia, Jake Varley, et al. Robots that ask for help: Uncertainty alignment for large language model planners. *arXiv preprint arXiv:2307.01928*, 2023.
- Yaniv Romano, Evan Patterson, and Emmanuel Candes. Conformalized quantile regression. *Advances in neural information processing systems*, 32, 2019.
- Mauricio Sadinle, Jing Lei, and Larry Wasserman. Least ambiguous set-valued classifiers with bounded error levels. *Journal of the American Statistical Association*, 114(525):223–234, 2019.
- Geethen Singh, Glenn Moncrieff, Zander Venter, Kerry Cawse-Nicholson, Jasper Slingsby, and Tamara B Robinson. Uncertainty quantification for probabilistic machine learning in earth observation using conformal prediction. *Scientific Reports*, 14(1):16166, 2024.
- Akshai Parakkal Sreenivasan, Aina Vaivade, Yassine Noui, Payam Emami Khoonsari, Joachim Burman, Ola Spjuth, and Kim Kultima. Conformal prediction enables disease course prediction and allows individualized diagnostic uncertainty in multiple sclerosis. *npj Digital Medicine*, 8(1):224, 2025.
- Ryan J Tibshirani, Rina Foygel Barber, Emmanuel Candes, and Aaditya Ramdas. Conformal prediction under covariate shift. *Advances in neural information processing systems*, 32, 2019.
- Vladimir Vovk, Alexander Gammerman, and Glenn Shafer. *Algorithmic Learning in a Random World*. Springer, 2005.
- Larry Wasserman. All of statistics. *Springer Texts in Statistics*, 2004.